Partitioning uncertainty in projections of Arctic sea ice

David B. Bonan
Environmental Science and Engineering, California Institute of Technology, Pasadena, California
E-mail: dbonan@caltech.edu

Flavio Lehner
Department of Earth and Atmospheric Sciences, Cornell University, Ithaca, New York
Climate and Global Dynamics Laboratory, National Center for Atmospheric Research, Boulder, Colorado

Marika M. Holland
Climate and Global Dynamics Laboratory, National Center for Atmospheric Research, Boulder, Colorado

Abstract. Improved knowledge of the contributing sources of uncertainty in projections of Arctic sea ice over the 21st century is essential for evaluating impacts of a changing Arctic environment. Here, we consider the role of internal variability, model structure and emissions scenario in projections of Arctic sea-ice area (SIA) by using six single model initial-condition large ensembles and a suite of models participating in Phase 5 of the Coupled Model Intercomparison Project. For projections of September Arctic SIA change, internal variability accounts for as much as 40-60% of the total uncertainty in the next decade, while emissions scenario dominates uncertainty toward the end of the century. Model structure accounts for approximately 60-70% of the total uncertainty by mid-century and declines to 30% at the end of the 21st century in the summer months. For projections of wintertime Arctic SIA change, internal variability contributes as much as 50-60% of the total uncertainty in the next decade and impacts total uncertainty at longer lead times when compared to the summertime. In winter, there exists a considerable scenario dependence of model uncertainty with relatively larger model uncertainty under strong forcing compared to weak forcing. At regional scales, the contribution of internal variability can vary widely and strongly depends on the calendar month and region. For wintertime SIA change in the GIN and Barents Seas, internal variability contributes approximately 60-70% to the total uncertainty over the coming decades and remains important much longer than in other regions. We further find that the relative contribution of internal variability to total uncertainty is state-dependent and increases as sea ice volume declines. These results demonstrate that internal variability is a significant source of uncertainty in projections of Arctic sea ice.

Keywords: *sea ice, climate change, uncertainty, projections*

Submitted to: *Environ. Res. Lett.*

1. Introduction

The rapid loss of Arctic sea ice over the last few decades has been one of the most iconic symbols of anthropogenic climate change. Since the beginning of the satellite record, September Arctic sea-ice extent (SIE) has decreased by approximately 50% (Stroeve and Notz, 2018) and experienced considerable thinning largely due to a lengthening of the melt season (Perovich and Polashenski, 2012; Stroeve et al., 2014). While state-of-the-art global climate models (GCMs) predict a decline of Arctic SIE throughout the 21st century, the exact amount of ice loss remains highly uncertain (Massonnet et al., 2012; Notz et al., 2020). Studies suggest that in the summertime the Arctic will most likely be "ice free" by the end of the 21st century (Jahn, 2018; Niederdrenk and Notz, 2018; Sigmond et al., 2018) and could possibly be ice free as early as 2050 (Jahn, 2018) or 2030 (Wang and Overland, 2009). To improve projections of Arctic sea ice, the relative importance of the sources of uncertainty need to be characterized and if possible reduced, particularly at regional scales (Eicken, 2013; Barnhart et al., 2016; Årthun et al., 2020).

Internal variability, which refers to natural fluctuations in climate that occur even in the absence of external forcing, has long been known as an important source of uncertainty in projections of future climate (Hawkins and Sutton, 2009; Deser et al., 2012, 2020; Lehner et al., 2020; Maher et al., 2020). These fluctuations — intrinsic to the climate system — have been shown to exert a strong influence on short-term trends in numerous climate variables, such as surface temperature (Wallace et al., 2012; Smoliak et al., 2015; Deser et al., 2016; Lehner et al., 2017), precipitation (Hawkins and Sutton, 2011; Deser et al., 2012), snowpack (Siler et al., 2019), glacier mass balance (Marzeion et al., 2014; Bonan et al., 2019; Roe et al., 2020), ocean biogeochemical properties (Lovenduski et al., 2016; Schlunegger et al., 2020), and sea ice (Kay et al., 2011; Swart et al., 2015; Jahn et al., 2016; Screen and Deser, 2019; Rosenblum and Eisenman, 2017; England et al., 2019; Ding et al., 2019; Landrum and Holland, 2020). Recent estimates suggest that internal variability has contributed to approximately 50% of the observed trend in September Arctic SIE decline since 1979 (Stroeve et al., 2007; Kay et al., 2011; Zhang, 2015; Ding et al., 2017, 2019) and has strongly controlled regional patterns of sea ice loss (England et al., 2019).

The large role of internal variability in determining changes to Arctic SIE over the observational record means the predictability of future Arctic SIE at decadal timescales could remain heavily influenced by internal variability. The advent of decadal prediction systems (e.g., Meehl et al., 2009, 2014) raises the question whether realistic physics together with proper initialization of observations can lead GCMs to successfully constrain this internal variability and result in skillful estimates of SIE at decadal lead times (Koenigk et al., 2012; Yang et al., 2016). Initial-value predictability of Arctic SIE has been shown to be regionally and seasonally dependent (Blanchard-Wrigglesworth

et al., 2011b; Bushuk et al., 2019), often only lasting a few years at most for total Arctic SIE (Blanchard-Wrigglesworth et al., 2011a; Guemas et al., 2016). Yet, using a suite of perfect model experiments (which quantify the upper limits of predictability), Yeager et al. (2015) showed that the rate of sea ice loss in the North Atlantic may slow down in the coming decades due to a reduction of ocean heat transport into the Arctic, which itself is highly predictable. Similarly, Koenigk et al. (2012) found a link between meridional overturning circulation and the potential predictability of decadal mean sea ice concentration in the North Atlantic — consistent with Yang et al. (2016). However, even if uncertainty due to internal variability cannot be reduced, understanding its magnitude will allow for better decision making in light of that uncertainty. This raises an important question: what is the relative role of internal variability in future projections of Arctic sea ice? Any accounting for the sources of uncertainty in projections of Arctic SIE must quantify the relative importance of each source at different spatial and temporal scales. For example, how important is internal variability for projections of Arctic sea ice 15 versus 30 years from now? Moreover, because models exhibit different magnitudes of internal variability in sea ice, both at pan-Arctic (e.g., Notz et al., 2020; Olonscheck and Notz, 2017) and regional scales (e.g., England et al., 2019; Topál et al., 2020), such quantification must sample the influence of model uncertainty in the estimate of internal variability itself.

To examine these questions we use an unprecedented suite of single model initial-condition large ensembles (SMILEs) from six fully-coupled GCMs. Due to their sample size, these SMILEs uniquely allow us to partition uncertainty in projections of Arctic sea-ice area (SIA) into the relative roles of internal variability, model structure, and emissions scenario at both Arctic-wide and regional spatial scales without relying on statistical representations of the forced response or internal variability (e.g., Lique et al., 2016). The SMILEs also allow us to quantify the influence of different estimates of internal variability, a feature of sea ice projection uncertainty that has received little attention. In what follows, we first investigate the role of internal variability in projections of total Arctic SIA change. We then explore how the relative partitioning of each source changes as a function of season and Arctic region and how this partitioning is influenced by the mean-state of Arctic sea ice.

2. Data

2.1. Observational data sets

Monthly Arctic SIA from 1979 to 2020 (2019 for December) was derived using observations of monthly sea ice concentration (SIC) from the National Snow and Ice Data Center passive microwave retrievals bootstrap algorithm (Comiso et al., 2017). A reconstruction of monthly Arctic SIA (Walsh et al., 2017) is used to analyze variability over a longer observational period. We choose to begin with the year 1930 from the

reconstruction to account for uncertainties and sparse data coverage prior to the 1930s.

2.2. MMLEA output

We use six SMILEs from the Multi-Model Large Ensemble Archive (MMLEA; Deser et al., 2020) to investigate the role of internal variability on projections of Arctic sea ice. These include the: 40 member Community Earth System Model Large Ensemble Community Project (CESM1-LE; Kay et al., 2015), 50 member Canadian Earth System Model Large Ensemble (CanESM2-LE; Kirchmeier-Young et al., 2017), 30 member Commonwealth Scientific and Industrial Research Organisation Large Ensemble (CSIRO-Mk3.6.0-LE; Jeffrey et al., 2013), 20 member Geophysical Fluid Dynamics Laboratory Large Ensemble (GFDL-CM3-LE; Sun et al., 2018), 30 member Geophysical Fluid Dynamics Laboratory Earth System Model Large Ensemble (GFDL-ESM2M-LE; Rodgers et al., 2015), and 100 member Max Planck Institute Grand Ensemble (MPI-GE; Maher et al., 2019). Each SMILE uses historical and RCP8.5 forcing. We also use the RCP2.6 and RCP4.5 100 member ensembles from the MPI-GE. From each SMILE we use SIC to compute monthly Arctic SIA for 6 Arctic regions and the pan-Arctic (see Figure S1). We also use sea ice thickness to compute monthly Arctic sea-ice volume (SIV) for these same spatial domains. Note that the output from GFDL-CM3 and GFDL-ESM2M is the average thickness over the ice-covered area of the grid cell. To compute SIV, the monthly averaged ice-covered thickness from both models was multiplied by the monthly average SIC of each cell to get the grid-cell average SIT. Prior to these calculations, all model output is regridded to a common $1^\circ \times 1^\circ$ analysis grid using nearest-neighbor interpolation. We choose SIA since SIE can be more grid-size dependent (Notz, 2014).

2.3. CMIP5 output

We use monthly output from the historical, RCP2.6, RCP4.5, and RCP8.5 simulations of 18 different GCMs participating in CMIP5 (Taylor et al., 2012). Since the historical simulations end in 2005, we merge the 1850-2005 fields from the historical simulations with the 2006-2100 fields under each RCP forcing scenario. For each experiment, we use SIC to compute monthly Arctic SIA. The set of GCMs evaluated reflects those that provide the necessary output for each RCP scenario (see Table S1). All model output is regridded to a common $1^\circ \times 1^\circ$ analysis grid using nearest-neighbor interpolation.

3. Uncertainty in projections of Arctic sea ice

We begin by partitioning three sources of uncertainty following Hawkins and Sutton (2009) and Lehner et al. (2020), where the total uncertainty (T) is the sum of the uncertainty due to model structure (M), the uncertainty due to internal variability (I) and the uncertainty due to emissions scenario (S). Each source can be estimated for a given time t and location x such that:

$$T(t,x) = I(t,x) + M(t,x) + S(t,x) \tag{1}$$

where the fractional uncertainty from a given source is calculated as I/T, M/T, and S/T. I is calculated as the variance across ensemble members of each SMILE, yielding one time-varying estimate of I per SMILE. Note, I is computed across RCP8.5 forcing scenarios only. Averaging across the six I yields the multi-model mean internal variability uncertainty (see upper bold white lines in Figure 1c and Figure 1d). To quantify the influence of model uncertainty in the estimate of I we also use the model with the largest and smallest I (see white shaded regions in Figure 1). Model uncertainty in the estimate of I has emerged as an important and potentially reducible source of uncertainty in regional temperature and precipitation changes (Lehner et al., 2020; Deser et al., 2020) and projections of global ocean biogeochemical properties (Schlunegger et al., 2020). M is calculated as the variance across the ensemble means of the six SMILEs under RCP8.5 forcing. It is important to note that the SMILEs used in this study are found to be reasonably representative of the CMIP5 inter-model spread for the percent of remaining Arctic sea ice cover (see Fig. 1 and Fig. S2), but a more systematic comparison is necessary before generalizing this conclusion. Finally, since only a few of the SMILEs were run with more than one emissions scenario, we turn to CMIP5 for S, which is calculated as the variance across the multi-model mean RCP scenarios (see Table S1 for details). We include CMIP5 models that contain all three forcing scenarios (RCP2.6, RCP4.5, RCP8.5) to mitigate the influence of model structure in the estimate of S. This resulted in 18 CMIP5 models (see Table S1). Prior to these variance calculations, the monthly SIA was smoothed with a 5-year running mean to isolate the effect of uncertainty on short-term projections and then used to calculate the percent of remaining sea ice relative to the mean of each simulation from 1995-2014 (see Figure S2) following Boé et al. (2009). Thus, importantly, this study examines "response" uncertainty relative to a reference period, which differs from absolute uncertainty. Focusing on response uncertainty rather than absolute uncertainty removes the confounding issue of model differences due to mean state biases and may also help elucidate why models have different sea ice sensitivities to carbon-dioxide and warming (Winton, 2011; Notz and Stroeve, 2016; Notz et al., 2020).

3.1. Total Arctic sea-ice area

We first consider projections of Arctic SIA change in September (the seasonal minimum) and March (the seasonal maximum). Figure 1 shows the fractional contribution of each source of uncertainty to total uncertainty. In September, uncertainty due to internal variability is important initially, accounting for approximately 40% of total uncertainty. However, over time model uncertainty increases and eventually dominates for the first half of the 21st century, before scenario uncertainty starts to dominate after approximately mid-century (Fig. 1c). However, model uncertainty in internal variability itself can have an effect on climate projections (e.g., Lehner et al., 2020). Accounting for the minimum and maximum contribution of internal variability to total uncertainty suggests that internal variability could account for as much as 40-60% or as little as 10-20% of

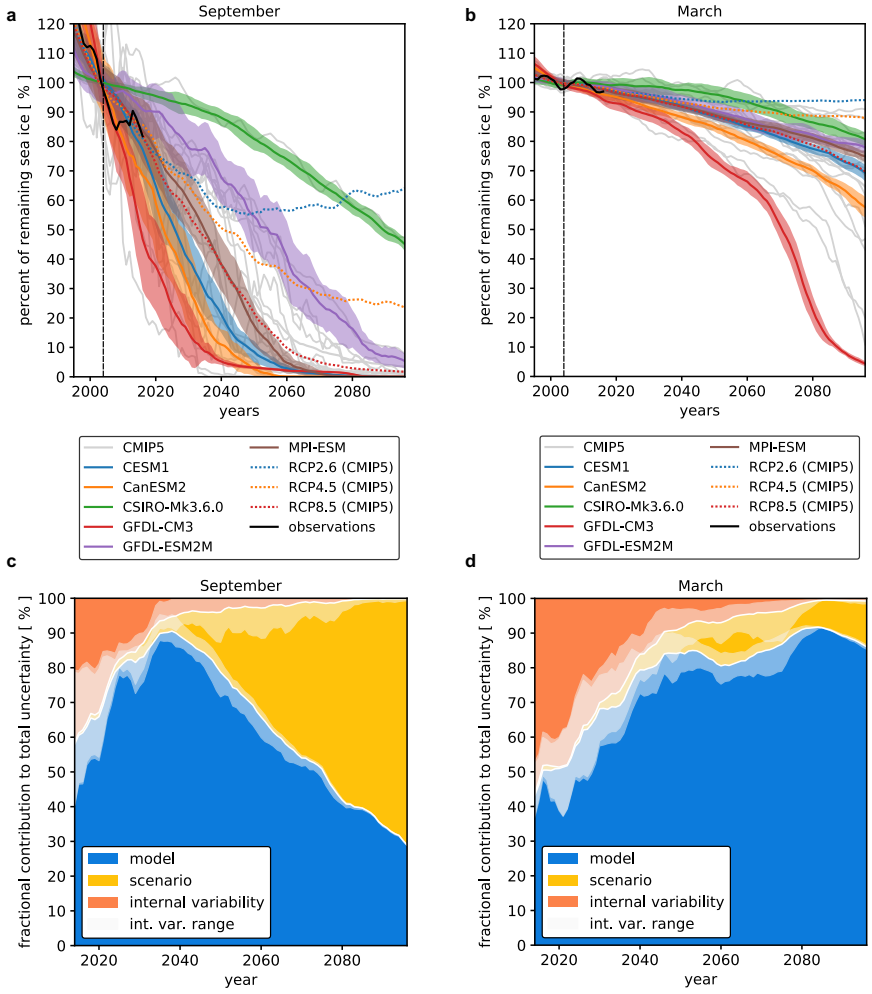

Figure 1. (a-b) Percent of remaining sea ice for each single-model initial condition large ensemble (SMILE) and the available CMIP5 output relative to 1995-2014 under historical and RCP8.5 forcing for (a) September and (b) March. Both panels are for five-year mean projections. The bold line represents the ensemble-mean of each SMILE and the shading represents the standard deviation of each SMILE under historical and RCP8.5 forcing. The colored dotted lines represent the multi-model mean of each RCP scenarios from 18 CMIP5 models. The grey lines represent the 18 CMIP5 models under RCP8.5. The black line denotes observations from 1979-2020. (c-d) Fractional contribution of model structure, emissions scenario, and internal variability to total uncertainty for the percent of remaining Arctic sea ice cover in (c) September and (d) March. The solid white lines denote the borders between each source of uncertainty, while the transparent white shading around those lines is the range of this estimate based on different estimates of internal variability in the MMLEA. Both fractional uncertainty panels are for five-year mean projections of percent of remaining Arctic sea-ice cover relative to 1995-2014.

total uncertainty in projections of September SIA change in the coming decades and could contribute approximately 10% throughout the 21st century. Note, these results are similar for most summer months and summertime averages (see Fig. S4 and S5).

A different story emerges for projections of Arctic SIA change in March. While uncertainty due to internal variability is again important initially and accounts for more of the total uncertainty at longer lead times, model uncertainty increases and quickly dominates until the end of the century (Fig. 1d). Scenario uncertainty is relatively less important for projections of Arctic SIA change in March and, more broadly, during the wintertime (see Fig. S4). This differs slightly from the results of Notz et al. (2020), which find a larger role for scenario uncertainty. These differences likely arise through our formulation of uncertainty due to emissions scenario and model structure as response uncertainty rather than absolute uncertainty. In winter, model uncertainty is large and diminishes scenario uncertainty in relative terms. Another caveat is that in winter the model uncertainty across SMILEs is larger and less representative of the model uncertainty across CMIP5 models. As a consequence, the relative contribution of scenario uncertainty in SMILEs is seemingly small and only about half of what it would be if model uncertainty had been taken from CMIP5 (see below for more discussion). Uncertainty in model internal variability remains large throughout the 21st century, suggesting internal variability could account for as much as 20% or as little as 5% of the total uncertainty beyond mid-century. The relative partitioning is similar for most winter months and wintertime averages (see Fig. S4 and S5).

We also calculate model uncertainty using CMIP5 models from the RCP2.6, RCP4.5 and RCP8.5 scenarios to examine the effect of weak forcing and thus weaker model response uncertainty for the late 21st century (see Fig. S6). To do this, we calculate the variance across models for each RCP scenario, which results in an estimate of model uncertainty for three RCP scenarios. This formulation of model uncertainty combines the influence of model uncertainty and internal variability, but we expect the confounding influence of internal variability to be very small across 2070-2100 averages. In general, we find only small differences in the estimate of model uncertainty for RCP8.5 and the SMILEs, suggesting these models are indeed representative of the CMIP5 models when compared for the same scenario. As discussed in the previous paragraph, in late winter, the contribution of scenario uncertainty to total uncertainty nearly doubles when using CMIP5 RCP8.5 instead of the SMILEs, likely reflecting the fact that the SMILEs are less representative of winter sea ice behavior when compared to the CMIP5 models. Furthermore, there is a clear scenario dependence of model uncertainty in winter months, with larger values for RCP8.5 than for RCP4.5 and RCP2.6 (see Fig. S6). At the end of the 21st century, model uncertainty estimated from RCP2.6 accounts for only 40% of the total uncertainty whereas from RCP8.5 it accounts for 90% of the total uncertainty. In summer, model uncertainty is similar across each RCP scenario (see Fig. S6) largely because model uncertainty is saturated as SIA goes to zero. Thus, there is an inherent

limitation in our formulation of M as it is strongly dependent on the emission scenario, particularly in winter when enough sea ice remains for model differences to become more clear under strong compared to weak radiative forcing. Furthermore, examining the uncertainty partitioning without 5-year running averages shows that the relative role of internal variability in projection uncertainty can increase by approximately 10-20% in the first decade across all months (see Fig. S7).

These results suggest that uncertainty in short-term projections of Arctic sea ice change, regardless of the season, is dominated by internal variability, while for long-term projections of Arctic sea ice, both scenario and model uncertainty become important. At long lead times, scenario uncertainty accounts for most of the uncertainty in projections of Arctic SIA change in the summer months and model uncertainty accounts for most of the uncertainty in projections of Arctic SIA change in the winter months. This likely reflects the fact that September Arctic SIA disappears in most GCMs by 2100 under RCP8.5.

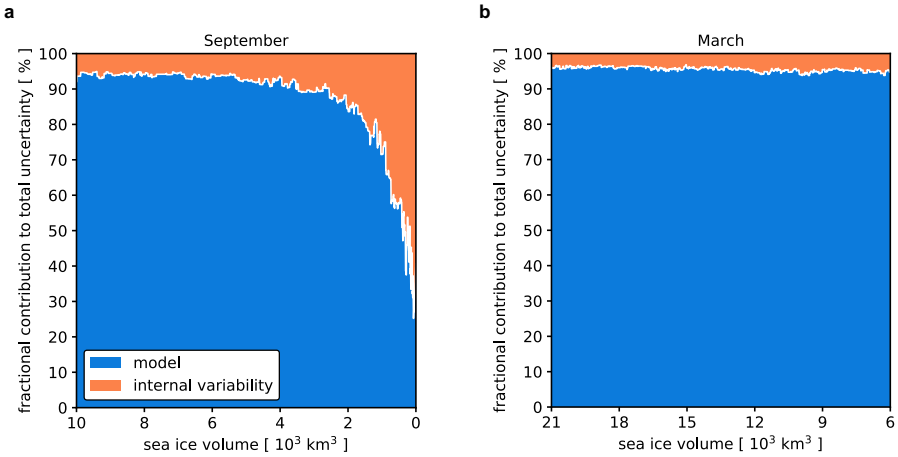

Figure 2. Fractional contribution of model structure and internal variability to total uncertainty for Arctic sea-ice area (SIA) in (a) September and (b) March as a function of Arctic sea-ice volume (SIV). The solid white lines denotes the border between the two sources of uncertainty. Both fractional uncertainty panels are for projections of Arctic SIA with no temporal averaging or reference period. Note the x-axis is different for (a) and (b).

3.2. State dependence of internal variability

These results show a clear time-scale dependence for the relative importance of internal variability in uncertainty of projections of Arctic SIA change. However, recent studies have shown that the internal variability and the predictability of Arctic sea ice can change over time and under anthropogenic forcing (Goosse et al., 2009; Mioduszewski et al., 2019; Holland et al., 2019). September Arctic SIA variability is expected to increase under warming (Goosse et al., 2009; Mioduszewski et al., 2019), suggesting that

the role of internal variability in sea ice projections is mean-state dependent. To investigate the role of internal variability in projections of Arctic sea ice as a function of the mean-state, we partition the relative sources of uncertainty with respect to SIV by binning a given SIA to its associated SIV for each month. We then perform the same variance analysis described above as a function of SIV instead of as a function of time. Doing this for each SMILE member and the ensemble-mean of each SMILE allows us to examine the contributing sources of uncertainty as a function of SIV.

Figure 2 shows the fractional contribution of internal variability and model structure to total uncertainty for future Arctic SIA in September and March as a function of September and March Arctic SIV, respectively. Note, scenario uncertainty was excluded in these calculations (by using simulations from RCP 8.5 only) to isolate the effect of internal variability at different mean-states with respect to model uncertainty under the same mean-state. In September, as SIV declines — which is expected to occur throughout the 21st century — internal variability remains constant for most SIV values, accounting for approximately 10% of total uncertainty. However, at lower SIV regimes ($< 3{,}000$ km^3), the contribution of internal variability increases and accounts for approximately 80% of the total uncertainty at low thickness sea ice regimes (i.e., SIV $<$ 1,000 km^3). This is consistent with previous work that has shown increased variability of summer Arctic SIA as it declines (e.g., Mioduszewski et al., 2019). Note, this result does not refer to when the maximum SIA variability occurs ($\approx$ 3-4 million km^2), but at which mean state the relative contribution of internal variability to projection uncertainty is largest. In March, the contribution of internal variability to total uncertainty remains relatively constant at all SIV regimes, likely reflecting the fact that sea ice is present in most winter climates in future projections (e.g., Goosse et al., 2009). It is important to note that this increase in the contribution of internal variability to uncertainty at lower SIV regimes holds for summer (June, July, and August) months (not shown).

3.3. Regional Arctic sea-ice area

While the loss of total Arctic SIA is important for understanding the global climate response, climate change and sea ice loss are experienced predominately at regional scales (Barnhart et al., 2014; Lehner and Stocker, 2015). To investigate uncertainty in regional SIA projections, we compute SIA for 6 Arctic regions, which include the Central Arctic, Siberian Marginal Seas, North American Marginal Seas, Baffin/Hudson Bay and the Labrador Sea, the Bering Sea and Sea of Okhotsk, and Greenland-Iceland-Norwegian (GIN) and Bering Seas. These regions were chosen to represent geographically distinct parts of the Arctic ocean, where SIA retreat occurs with different velocities. As with total Arctic SIA change, the SMILEs used in this study are found to be reasonably representative of the CMIP5 inter-model spread for the percent of remaining Arctic sea ice cover in each region (see Figure S3).

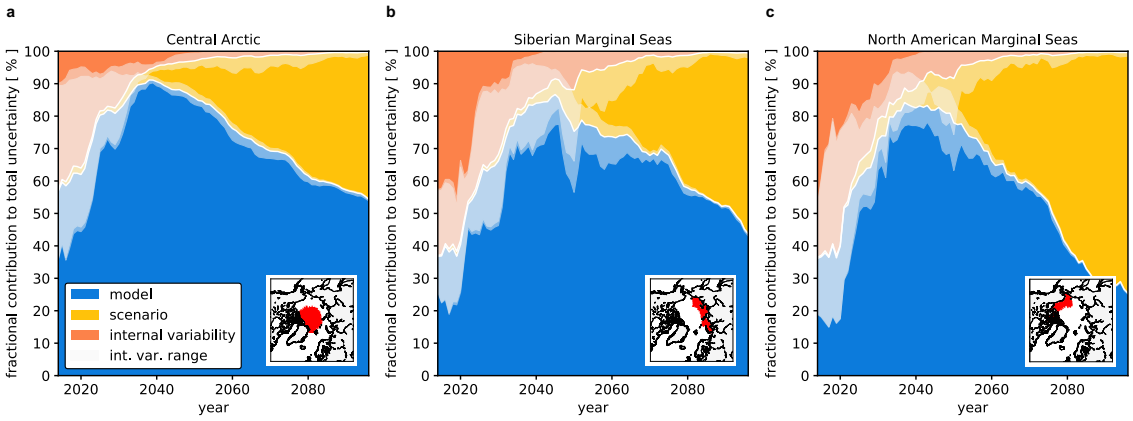

Figure 3. Fractional contribution of model structure, emissions scenario, and internal variability to total uncertainty for percent of remaining sea ice cover in July, August and September (JAS) for the Central Arctic, Siberian Marginal Seas (Kara Sea, Laptev Sea, East Siberian Sea), and North American Marginal Seas (Chukchi Sea, Beaufort Sea, Canadian Archipelago). The solid white lines indicate the borders between sources of uncertainty, while the transparent white shading around those lines is the range of this estimate based on different estimates of internal variability in the MMLEA. All panels are for five-year mean projections of percent of remaining Arctic sea-ice cover relative to 1995-2014.

Figure 3 shows the fractional contribution of each source of uncertainty to total uncertainty in projections of July, August, and September (JAS) SIA change in the Central Arctic (Fig. 3a), Siberian Marginal Seas (Fig. 3b), and North American Marginal Seas (Fig. 3c). We only show summertime SIA change as these regions are fully ice covered in the wintertime and exhibit little wintertime variability throughout much of the 21st century. As with total September Arctic SIA change, there is a large role for internal variability initially, accounting for approximately 40% of total uncertainty in the Central Arctic (Fig. 3a) and 60% in the Siberian and North American Marginal Seas (Fig. 3b and 3c). However, over time model uncertainty increases and eventually dominates for the first half of the 21st century in Central Arctic (Fig. 3a) and marginal seas (Fig. 3b and Fig. 3c), accounting for 60-70% of the total uncertainty. Note, the contribution of model structure to total uncertainty at the end of the century is lowest for the North American Marginal Seas. By the end of the 21st century scenario uncertainty dominates and accounts for over half of the uncertainty, meaning that whether or not an ice free Arctic occurs in the summertime is a direct consequence of climate change policy. Notably, the inter-model range of simulated internal variability contributions remains larger through the 21st century in each region when compared to total Arctic SIA change.

Figure 4 shows the fractional contribution of each source of uncertainty to total uncertainty in projections of January, February, and March (JFM) Arctic SIA change in Baffin Bay, Hudson Bay and the Labrador Sea (Fig. 4a), Bering Sea and Sea of Okhotsk

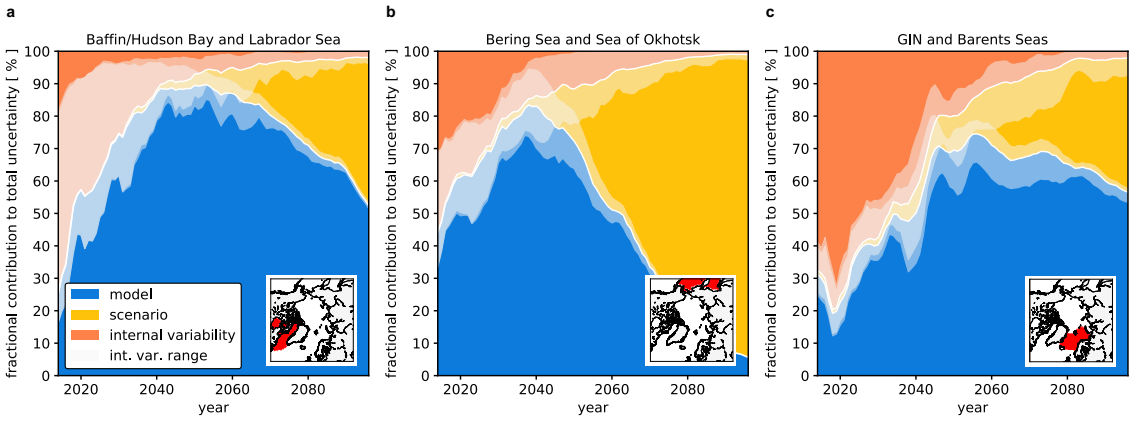

Figure 4. Fractional contribution of model structure, emissions scenario, and internal variability to total uncertainty for percent of remaining sea ice cover in January, February, and March (JFM) for (a) Baffin Bay, Hudson Bay, and the Labrador Sea, (b) Being Sea and Sea of Okhotsk, and the (c) GIN and Barents Seas. The solid white lines indicate the borders between sources of uncertainty, while the transparent white shading around those lines is the range of this estimate based on different estimates of internal variability in the MMLEA. All panels are for five-year mean projections of percent of remaining Arctic sea-ice cover relative to 1995-2014.

(Fig. 4b), and GIN and Barents Seas (Fig. 4c). These regions were selected to examine wintertime SIA change as there is highly variable SIA in winter and little-to-no SIA in summer. As with regions of variable summer sea ice cover, these regions show a distinct pattern of uncertainty partitioning. For Baffin Bay, Hudson Bay, and Labrador Sea, approximately 80% of total uncertainty in the next decade is attributable to internal variability. Note that the contribution of uncertainty in the estimate of internal variability itself can cause this to change to only 20% (mainly driven by CSIRO-Mk3.6.0 which exhibits less internal variability of SIA). The internal variability contribution diminishes to approximately 10% by the end of the century, and model structure dominates by 2030. A similar picture emerges for the Bering Sea and Sea of Okhotsk, but instead scenario uncertainty dominates in the latter half of the 21st century. Interestingly, the uncertainty partitioning for the GIN and Barents Seas has a distinct structure: internal variability dominates projection uncertainty for the next 30 years and remains persistent throughout much of the 21st century. The contribution of internal variability is notably larger than in other regions and is most likely related to the influence of Atlantic heat transport on sea ice (Årthun et al., 2012). This contribution also suggests that since sea-surface temperature is much more predictable in the North Atlantic when compared to other regions on decadal timescales (Pohlmann et al., 2004), so too is Arctic sea ice. Another explanation for the larger role of internal variability could be that Atlantic multidecadal variability is thought to play a primary role in determining the sea ice edge in this region, particularly in winter when it reaches into the zone of influence of multidecadal North Atlantic sea-surface temperature variability (Goessling et al., 2016).

A key result here — in contrast to total Arctic SIA change for March and September — is the larger role of internal variability in contributing to total uncertainty, which persists throughout much of the 21st century. This suggests decadal predictions of regional Arctic SIA will be highly influenced by internal variability, especially for wintertime conditions in the GIN and Barents Seas — consistent with Årthun et al. (2020). Moreover, the range of internal variability across models presents a unique challenge as internal variability could account for as much as 80% or as little as 20% of the total uncertainty in regions like the Labrador Sea in the coming decades. Understanding the cause of the range in this internal variability uncertainty is an important next step, whether it is related to model biases in the representation of Atlantic multidecadal variability or dependent on the sea ice mean-state.

3.4. Reducing the inter-model spread of internal variability

A unique result of this analysis is the partitioning of uncertainty due to different estimates of internal variability, which varies considerably across GCMs (see Figure 1). This suggests that at least some GCMs are biased in their magnitude of variability. Due to the short observational record, it is difficult to precisely estimate the real-world magnitude of SIA internal variability (e.g., Brennan et al., 2020). However, using a reconstruction of September Arctic SIA back to 1930 (Walsh et al., 2017) we try to estimate historical Arctic SIA variability. To do this, we calculate non-overlapping 5-year trends of September Arctic SIA in observations and models. Figure 5 shows histograms of separate 5-year trends in September Arctic SIA from 1950-2019 using all members of each SMILE. A 4th order polynomial was used to approximate and remove the forced response consistently in both observations and models. The grey bars indicate the range from Walsh et al. (2017) using separate 5-year trends from 1930 to 2019. While most models appear to span the range of internal variability in the historical record, CSIRO-Mk3.6.0 does not simulate a large enough range of 5-year trends, most likely reflecting the fact that sea ice is biased high throughout the summer. This suggests the lowest contribution of internal variability to total uncertainty in projections September Arctic SIA change seen earlier in the paper is likely not realistic. Understanding and resolving these biases in internal variability across fully-coupled GCMs should remain a focus of the sea ice community as it is important for attribution of observed sea ice loss to anthropogenic climate change as well as for efforts of decadal prediction.

4. Concluding remarks

The impacts of Arctic sea ice loss will be predominately felt by coastal communities, making it crucial to quantify and reduce projection uncertainty at regional scales. Here, we used a suite of SMILEs to investigate the sources of uncertainty in projections of Arctic SIA change. For September SIA change, model structure contributes between 30-80% of the total uncertainty over the next century, while for March SIA change,

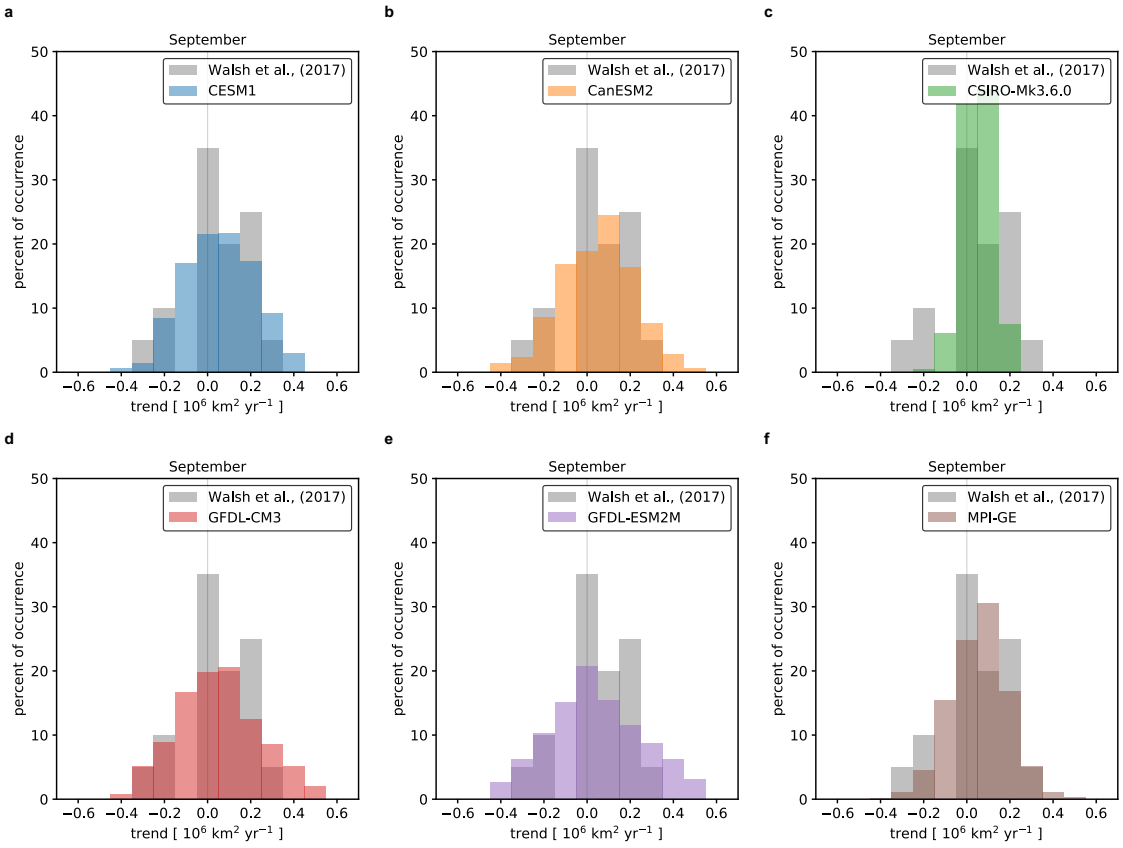

Figure 5. Percent of occurrence of non-overlapping 5-year trends in September Arctic sea-ice area (SIA) from 1950-2019 for the (a) CESM1, (b) CanESM2, (c) CSIRO-Mk3.6.0, (d) GFDL-CM3, (e) GFDL-ESM2M, and (f) MPI-ESM. A 4th order polynomial was removed from each member of each SMILE prior to trend calculations to estimate the forced response. The bars show the distribution of trends for all members. The grey bars show percent of occurrence of non-overlapping 5-year trends in September Arctic SIA from 1930-2017 as estimated from Walsh et al. (2017). A 4th order polynomial was also removed from the dataset prior to trend calculations to estimate the forced response.

model structure contributes approximately 40-80% of the total uncertainty over the next century and accounts for more uncertainty at the end of the 21st century. We find a clear timescale dependence for internal variability. For September SIA change, internal variability contributes approximately 40-60% of total uncertainty in the next few decades, while for March SIA change — and winter SIA change more generally — internal variability contributes between 50-60% of total uncertainty and influences projections at longer lead times. Scenario uncertainty contributes mainly to uncertainty in summertime projections, accounting for approximately 70% of total uncertainty by the end of the century. The smaller contribution of scenario uncertainty to total uncertainty in winter likely reflects the fact that model uncertainty is so large that it diminishes scenario uncertainty in relative terms. It is important to note that in winter model uncertainty strongly depends on the emissions scenario used to calculate it, which may also

affect estimates of the relative role of scenario uncertainty (see Fig. S6). We also find that the role for internal variability is mean-state dependent with thinner summer sea ice regimes more heavily influenced by internal variability, accounting for approximately 80% of total uncertainty for SIV $<$ 1,000 km^3. At regional scales, the contribution of internal variability to total uncertainty increases, but has a large range and strongly depends on the month and region. In the GIN and Barents Seas, for instance, internal variability contributes approximately 50-70% of the total uncertainty over the next 30 years, while for the Central Arctic, internal variability accounts for approximately 20-30% of the total uncertainty. This is likely related to the influence of Atlantic heat transport on sea ice in the North Atlantic during the wintertime and multidecadal variability of North Atlantic sea-surface temperature.

An important result of this study is the inter-model spread in the contribution of internal variability to projection uncertainty. Recent work has highlighted the role of remote internal processes in determining sea ice trends across these same SMILEs (Topál et al., 2020), but a more process-oriented analysis of the spatial and temporal timescales of this variability may better reveal the sources of inter-model spread. For instance, it has been shown that these remote processes are not stable on longer time scales (Bonan and Blanchard-Wrigglesworth, 2020), suggesting that associated variability in September SIA during the satellite era does not paint a complete picture of the future SIA variability. The outsized role for internal variability in projections of Arctic sea ice changes in the coming decades further motivates the use of SMILEs to investigate a wide range of possible sequences of sea ice internal variability and its drivers. However, such work is beyond the scope of this paper, whose primary goal is to highlight the relative contribution of different sources of uncertainty to Arctic sea ice projections at different spatial and temporal scales.

While internal variability poses a great challenge for predicting Arctic SIA in the coming decades, the contribution of model structure to total uncertainty should not be ignored. So-called "emergent constraints", which link the inter-model spread in climate projections to observable predictors, should be used when characterizing projection uncertainty. Indeed, model uncertainty has been reduced through observational constraints. Previous work has related the amount of future ice loss to the magnitude of historical SIA trends (Boé et al., 2009; Hall et al., 2019) and to the initial state of the sea ice (Bitz, 2008; Massonnet et al., 2012; Hall et al., 2019) and the Arctic climate (Senftleben et al., 2020), but open questions remain as to why these relationships exist and persist throughout the next century. Further comparison of new and old generations of climate models may better reveal the sources of this spread. Understanding biases in these trends (e.g., Rosenblum and Eisenman, 2016, 2017) and the physical mechanisms behind these constraints will improve the reliability of sea ice projections and increase confidence in our understanding of what controls the rate of Arctic sea ice loss.

Acknowledgements

The authors thank the US CLIVAR Working Group on Large Ensembles for making the output publicly available, which can be found at the Multi-Model Large Ensemble Archive (http://www.cesm.ucar.edu/projects/community-projects/MMLEA/). The authors also thank the climate modeling groups for producing and making available their output, which is accessible at the Earth System Grid Federation (ESGF) Portal (https://esgf-node.llnl.gov/search/cmip5/). This work was greatly improved through discussions with Mitch Bushuk and comments from Tapio Schneider and Katie Brennan. The authors are grateful for helpful comments from Dirk Notz and one anonymous reviewer, as well as the Editor. D.B.B. was supported by an American Meteorological Society (AMS) Graduate Fellowship. F.L. was supported by the Swiss National Science Foundation Ambizione Fellowship (Project PZ00P2_174128) and the Regional and Global Model Analysis (RGMA) component of the Earth and Environmental System Modeling Program of the U.S. Department of Energys Office of Biological & Environmental Research (BER) via NSF IA 1844590. Contributions from M.M.H. were supported by the National Center for Atmospheric Research (NCAR), which is a major facility sponsored by the NSF under Cooperative Agreement No. 1852977.

References

1. Årthun, M., Eldevik, T., Smedsrud, L., Skagseth, Ø., and Ingvaldsen, R. (2012). Quantifying the influence of Atlantic heat on Barents Sea ice variability and retreat. *Journal of Climate*, 25(13):4736–4743.
2. Årthun, M., Onarheim, I. H., Dörr, J., and Eldevik, T. (2020). The seasonal and regional transition to an ice-free Arctic. *Geophysical Research Letters*, 48(1):e2020GL090825.
3. Barnhart, K. R., Miller, C. R., Overeem, I., and Kay, J. E. (2016). Mapping the future expansion of Arctic open water. *Nature Climate Change*, 6(3):280–285.
4. Barnhart, K. R., Overeem, I., and Anderson, R. S. (2014). The effect of changing sea ice on the physical vulnerability of Arctic coasts. *Cryosphere*, 8(5).
5. Bitz, C. M. (2008). Some aspects of uncertainty in predicting sea ice thinning. *Arctic Sea Ice Decline: Observations, Projections, Mechanisms, and Implications, Geophys. Monogr*, 180:63–76.
6. Blanchard-Wrigglesworth, E., Armour, K. C., Bitz, C. M., and DeWeaver, E. (2011a). Persistence and inherent predictability of Arctic sea ice in a GCM ensemble and observations. *Journal of Climate*, 24(1):231–250.
7. Blanchard-Wrigglesworth, E., Bitz, C., and Holland, M. (2011b). Influence of initial conditions and climate forcing on predicting Arctic sea ice. *Geophysical Research Letters*, 38(18).
8. Boé, J., Hall, A., and Qu, X. (2009). September sea-ice cover in the Arctic Ocean projected to vanish by 2100. *Nature Geoscience*, 2(5):341–343.
9. Bonan, D. B. and Blanchard-Wrigglesworth, E. (2020). Nonstationary teleconnection between the Pacific Ocean and Arctic sea ice. *Geophysical Research Letters*, 47(2):e2019GL085666.
10. Bonan, D. B., Christian, J. E., and Christianson, K. (2019). Influence of North Atlantic climate variability on glacier mass balance in Norway, Sweden and Svalbard. *Journal of Glaciology*, 65(252):580–594.

11. Brennan, M. K., Hakim, G. J., and Blanchard-Wrigglesworth, E. (2020). Arctic Sea-Ice Variability During the Instrumental Era. *Geophysical Research Letters*, 47(7):e2019GL086843.

12. Bushuk, M., Msadek, R., Winton, M., Vecchi, G., Yang, X., Rosati, A., and Gudgel, R. (2019). Regional Arctic sea–ice prediction: potential versus operational seasonal forecast skill. *Climate Dynamics*, 52(5-6):2721–2743.

13. Deser, C., Lehner, F., Rodgers, K., Ault, T., Delworth, T., DiNezio, P., Fiore, A., Frankignoul, C., Fyfe, J., Horton, D., et al. (2020). Insights from Earth system model initial-condition large ensembles and future prospects. *Nature Climate Change*, pages 1–10.

14. Deser, C., Phillips, A., Bourdette, V., and Teng, H. (2012). Uncertainty in climate change projections: the role of internal variability. *Climate dynamics*, 38(3-4):527–546.

15. Deser, C., Terray, L., and Phillips, A. S. (2016). Forced and internal components of winter air temperature trends over North America during the past 50 years: Mechanisms and implications. *Journal of Climate*, 29(6):2237–2258.

16. Ding, Q., Schweiger, A., LHeureux, M., Battisti, D. S., Po-Chedley, S., Johnson, N. C., Blanchard-Wrigglesworth, E., Harnos, K., Zhang, Q., Eastman, R., et al. (2017). Influence of high-latitude atmospheric circulation changes on summertime Arctic sea ice. *Nature Climate Change*, 7(4):289–295.

17. Ding, Q., Schweiger, A., LHeureux, M., Steig, E. J., Battisti, D. S., Johnson, N. C., Blanchard-Wrigglesworth, E., Po-Chedley, S., Zhang, Q., Harnos, K., et al. (2019). Fingerprints of internal drivers of Arctic sea ice loss in observations and model simulations. *Nature Geoscience*, 12(1):28–33.

18. Eicken, H. (2013). Arctic sea ice needs better forecasts. *Nature*, 497(7450):431–433.

19. England, M., Jahn, A., and Polvani, L. (2019). Nonuniform contribution of internal variability to recent Arctic sea ice loss. *Journal of Climate*, 32(13):4039–4053.

20. Goessling, H. F., Tietsche, S., Day, J. J., Hawkins, E., and Jung, T. (2016). Predictability of the Arctic sea ice edge. *Geophysical Research Letters*, 43(4):1642–1650.

21. Goosse, H., Arzel, O., Bitz, C. M., de Montety, A., and Vancoppenolle, M. (2009). Increased variability of the Arctic summer ice extent in a warmer climate. *Geophysical Research Letters*, 36(23).

22. Guemas, V., Blanchard-Wrigglesworth, E., Chevallier, M., Day, J. J., Déqué, M., Doblas-Reyes, F. J., Fučkar, N. S., Germe, A., Hawkins, E., Keeley, S., et al. (2016). A review on Arctic sea-ice predictability and prediction on seasonal to decadal time-scales. *Quarterly Journal of the Royal Meteorological Society*, 142(695):546–561.

23. Hall, A., Cox, P., Huntingford, C., and Klein, S. (2019). Progressing emergent constraints on future climate change. *Nature Climate Change*, 9(4):269–278.

24. Hawkins, E. and Sutton, R. (2009). The potential to narrow uncertainty in regional climate predictions. *Bulletin of the American Meteorological Society*, 90(8):1095–1108.

25. Hawkins, E. and Sutton, R. (2011). The potential to narrow uncertainty in projections of regional precipitation change. *Climate Dynamics*, 37(1-2):407–418.

26. Holland, M. M., Landrum, L., Bailey, D., and Vavrus, S. (2019). Changing Seasonal Predictability of Arctic Summer Sea Ice Area in a Warming Climate. *Journal of Climate*, 32(16):4963–4979.

27. Jahn, A. (2018). Reduced probability of ice-free summers for 1.5 C compared to 2 C warming. *Nature Climate Change*, 8(5):409–413.

28. Jahn, A., Kay, J. E., Holland, M. M., and Hall, D. M. (2016). How predictable is the timing of a summer ice-free Arctic? *Geophysical Research Letters*, 43(17):9113–9120.

29. Jeffrey, S., Rotstayn, L., Collier, M., Dravitzki, S., Hamalainen, C., Moeseneder, C., Wong, K., and Syktus, J. (2013). Australias CMIP5 submission using the CSIRO-Mk3. 6 model. *Aust. Meteor. Oceanogr. J*, 63:1–13.

30. Kay, J. E., Deser, C., Phillips, A., Mai, A., Hannay, C., Strand, G., Arblaster, J. M., Bates, S., Danabasoglu, G., Edwards, J., et al. (2015). The Community Earth System Model (CESM) large ensemble project: A community resource for studying climate change in the presence of internal climate variability. *Bulletin of the American Meteorological Society*, 96(8):1333–1349.

31. Kay, J. E., Holland, M. M., and Jahn, A. (2011). Inter-annual to multi-decadal Arctic sea ice extent trends in a warming world. *Geophysical Research Letters*, 38(15).

32. Kirchmeier-Young, M. C., Zwiers, F. W., and Gillett, N. P. (2017). Attribution of extreme events in Arctic sea ice extent. *Journal of Climate*, 30(2):553–571.

33. Koenigk, T., Beatty, C. K., Caian, M., Döscher, R., and Wyser, K. (2012). Potential decadal predictability and its sensitivity to sea ice albedo parameterization in a global coupled model. *Climate dynamics*, 38(11-12):2389–2408.

34. Landrum, L. and Holland, M. M. (2020). Extremes become routine in an emerging new Arctic. *Nautre Climate Change*, (https://doi.org/10.1038/s41558-020-0892-z).

35. Lehner, F., Deser, C., Maher, N., Marotzke, J., Fischer, E. M., Brunner, L., Knutti, R., and Hawkins, E. (2020). Partitioning climate projection uncertainty with multiple large ensembles and CMIP5/6. *Earth System Dynamics*, 11(2):491–508.

36. Lehner, F., Deser, C., and Terray, L. (2017). Toward a new estimate of time of emergence of anthropogenic warming: Insights from dynamical adjustment and a large initial-condition model ensemble. *Journal of Climate*, 30(19):7739–7756.

37. Lehner, F. and Stocker, T. F. (2015). From local perception to global perspective. *Nature Climate Change*, 5(8):731–734.

38. Lique, C., Holland, M. M., Dibike, Y. B., Lawrence, D. M., and Screen, J. A. (2016). Modeling the Arctic freshwater system and its integration in the global system: Lessons learned and future challenges. *Journal of Geophysical Research: Biogeosciences*, 121(3):540–566.

39. Lovenduski, N. S., McKinley, G. A., Fay, A. R., Lindsay, K., and Long, M. C. (2016). Partitioning uncertainty in ocean carbon uptake projections: Internal variability, emission scenario, and model structure. *Global Biogeochemical Cycles*, 30(9):1276–1287.

40. Maher, N., Lehner, F., and Marotzke, J. (2020). Quantifying the role of internal variability in the climate we will observe in the coming decades. *Environmental Research Letters*, 15.

41. Maher, N., Milinski, S., Suarez-Gutierrez, L., Botzet, M., Kornblueh, L., Takano, Y., Kröger, J., Ghosh, R., Hedemann, C., Li, C., et al. (2019). The Max Planck Institute grand ensemble-enabling the exploration of climate system variability. *Journal of Advances in Modeling Earth Systems*, 11:2050–2069.

42. Marzeion, B., Cogley, J. G., Richter, K., and Parkes, D. (2014). Attribution of global glacier mass loss to anthropogenic and natural causes. *Science*, 345(6199):919–921.

43. Massonnet, F., Fichefet, T., Goosse, H., Bitz, C. M., Philippon-Berthier, G., Holland, M. M., and Barriat, P.-Y. (2012). Constraining projections of summer Arctic sea ice. *The Cryosphere*, 6(6):1383–1394.

44. Meehl, G. A., Goddard, L., Boer, G., Burgman, R., Branstator, G., Cassou, C., Corti, S., Danabasoglu, G., Doblas-Reyes, F., Hawkins, E., et al. (2014). Decadal climate prediction: an update from the trenches. *Bulletin of the American Meteorological Society*, 95(2):243–267.

45. Meehl, G. A., Goddard, L., Murphy, J., Stouffer, R. J., Boer, G., Danabasoglu, G., Dixon, K., Giorgetta, M. A., Greene, A. M., Hawkins, E., et al. (2009). Decadal prediction: Can it be skillful? *Bulletin of the American Meteorological Society*, 90(10):1467–1486.

46. Mioduszewski, J. R., Vavrus, S., Wang, M., Holland, M., and Landrum, L. (2019). Past and future interannual variability in Arctic sea ice in coupled climate models. *Cryosphere*, 13(1).

47. Niederdrenk, A. L. and Notz, D. (2018). Arctic sea ice in a 1.5 C warmer world. *Geophysical Research Letters*, 45(4):1963–1971.

48. Notz, D. (2014). Sea-ice extent and its trend provide limited metrics of model performance. *The Cryosphere*, 8:229–243.
49. Notz, D. and Stroeve, J. (2016). Observed Arctic sea-ice loss directly follows anthropogenic CO2 emission. *Science*, 354(6313):747–750.
50. Notz et al. (2020). Arctic Sea Ice in CMIP6. *Geophysical Research Letters*, 47(10):e2019GL086749.
51. Olonscheck, D. and Notz, D. (2017). Consistently estimating internal climate variability from climate model simulations. *Journal of Climate*, 30(23):9555–9573.
52. Perovich, D. K. and Polashenski, C. (2012). Albedo evolution of seasonal Arctic sea ice. *Geophysical Research Letters*, 39(8).
53. Pohlmann, H., Botzet, M., Latif, M., Roesch, A., Wild, M., and Tschuck, P. (2004). Estimating the decadal predictability of a coupled AOGCM. *Journal of Climate*, 17(22):4463–4472.
54. Rodgers, K. B., Lin, J., and Frölicher, T. L. (2015). Emergence of multiple ocean ecosystem drivers in a large ensemble suite with an Earth system model. *Biogeosciences*, 12(11):3301–3320.
55. Roe, G. H., Christian, J. E., and Marzeion, B. (2020). On the attribution of industrial-era glacier mass loss to anthropogenic climate change. *The Cryosphere Discussions*, pages 1–27.
56. Rosenblum, E. and Eisenman, I. (2016). Faster Arctic sea ice retreat in CMIP5 than in CMIP3 due to volcanoes. *Journal of Climate*, 29(24):9179–9188.
57. Rosenblum, E. and Eisenman, I. (2017). Sea ice trends in climate models only accurate in runs with biased global warming. *Journal of Climate*, 30(16):6265–6278.
58. Schlunegger, S., Rodgers, K. B., Sarmiento, J. L., Ilyina, T., Dunne, J., Takano, Y., Christian, J., Long, M. C., Frölicher, T. L., Slater, R., et al. (2020). Time of Emergence & Large Ensemble intercomparison for ocean biogeochemical trends. *Global Biogeochemical Cycles*, page e2019GB006453.
59. Screen, J. and Deser, C. (2019). Pacific Ocean variability influences the time of emergence of a seasonally ice-free Arctic Ocean. *Geophysical Research Letters*, 46(4):2222–2231.
60. Senftleben, D., Lauer, A., and Karpechko, A. (2020). Constraining uncertainties in CMIP5 projections of September Arctic sea ice extent with observations. *Journal of Climate*, 33(4):1487–1503.
61. Sigmond, M., Fyfe, J. C., and Swart, N. C. (2018). Ice-free Arctic projections under the Paris Agreement. *Nature Climate Change*, 8(5):404–408.
62. Siler, N., Proistosescu, C., and Po-Chedley, S. (2019). Natural variability has slowed the decline in western US snowpack since the 1980s. *Geophysical Research Letters*, 46(1):346–355.
63. Smoliak, B. V., Wallace, J. M., Lin, P., and Fu, Q. (2015). Dynamical adjustment of the Northern Hemisphere surface air temperature field: Methodology and application to observations. *Journal of Climate*, 28(4):1613–1629.
64. Stroeve, J., Holland, M. M., Meier, W., Scambos, T., and Serreze, M. (2007). Arctic sea ice decline: Faster than forecast. *Geophysical research letters*, 34(9).
65. Stroeve, J., Markus, T., Boisvert, L., Miller, J., and Barrett, A. (2014). Changes in Arctic melt season and implications for sea ice loss. *Geophysical Research Letters*, 41(4):1216–1225.
66. Stroeve, J. and Notz, D. (2018). Changing state of Arctic sea ice across all seasons. *Environmental Research Letters*, 13(10):103001.
67. Sun, L., Alexander, M., and Deser, C. (2018). Evolution of the global coupled climate response to Arctic sea ice loss during 1990–2090 and its contribution to climate change. *Journal of Climate*, 31(19):7823–7843.
68. Swart, N. C., Fyfe, J. C., Hawkins, E., Kay, J. E., and Jahn, A. (2015). Influence of internal variability on Arctic sea-ice trends. *Nature Climate Change*, 5(2):86–89.

69. Taylor, K. E., Stouffer, R. J., and Meehl, G. A. (2012). An overview of CMIP5 and the experiment design. *Bulletin of the American Meteorological Society*, 93(4):485–498.

70. Topál, D., Ding, Q., Mitchell, J., Baxter, I., Herein, M., Haszpra, T., Luo, R., and Li, Q. (2020). An Internal Atmospheric Process Determining Summertime Arctic Sea Ice Melting in the Next Three Decades: Lessons Learned from Five Large Ensembles and Multiple CMIP5 Climate Simulations. *Journal of Climate*, 33(17):7431–7454.

71. Wallace, J. M., Fu, Q., Smoliak, B. V., Lin, P., and Johanson, C. M. (2012). Simulated versus observed patterns of warming over the extratropical Northern Hemisphere continents during the cold season. *Proceedings of the National Academy of Sciences*, 109(36):14337–14342.

72. Walsh, J. E., Fetterer, F., Scott Stewart, J., and Chapman, W. L. (2017). A database for depicting Arctic sea ice variations back to 1850. *Geographical Review*, 107(1):89–107.

73. Wang, M. and Overland, J. E. (2009). A sea ice free summer Arctic within 30 years? *Geophysical research letters*, 36(7).

74. Winton, M. (2011). Do climate models underestimate the sensitivity of Northern Hemisphere sea ice cover? *Journal of Climate*, 24(15):3924–3934.

75. Yang, C.-Y., Liu, J., Hu, Y., Horton, R. M., Chen, L., and Cheng, X. (2016). Assessment of Arctic and Antarctic sea ice predictability in CMIP5 decadal hindcasts. *Cryosphere*, 10(5):2429–2452.

76. Yeager, S. G., Karspeck, A. R., and Danabasoglu, G. (2015). Predicted slowdown in the rate of Atlantic sea ice loss. *Geophysical Research Letters*, 42(24):10–704.

77. Zhang, R. (2015). Mechanisms for low-frequency variability of summer Arctic sea ice extent. *Proceedings of the National Academy of Sciences*, 112(15):4570–4575.